Journal of Nuclear and Radiochemical Sciences, Vol. 17, pp. 23-29, 2017

Articles

Mössbauer Characterization of Iron in Ancient Buried Trees Excavated from the Foothills of Mt. Chokai

Shigeru Yamauchi[a,*], Yasuji Kurimoto[a], and Yoichi Sakai[b]

[a]*Institute of Wood Technology, Akita Prefectural University, Noshiro, Akita 016-0876, Japan*
[b]*Department of Chemistry, Daido University, Nagoya, Aichi 457-8530, Japan*

Received August 18, 2017; Accepted December 26, 2017; Published online January 25, 2018

The oxidation number and spin state of Fe in sample of ancient trees (*umoregi* trees) excavated from the foothills of Mt. Chokai in Japan were determined from the ^{57}Fe Mössbauer spectra. Moreover, basic structures of the Fe compounds were investigated using Mössbauer spectroscopy and complementary analytical techniques. The *umoregi* wood samples were prepared from the trunks of four tree species: Japanese cedar and Japanese zelkova which were brown and dark green, respectively; and Japanese oak and Japanese chestnut which were a pure black tone. Treatment with oxalic acid removed these characteristic colors from the samples. Mössbauer spectra were recorded at 293 K and 78 K, and their absorption line-shapes were analyzed using a curve-fitting method. At 293 K and 78 K, the respective isomer shifts of Fe were in the range of 0.21(3)-0.43(1) mm/s and 0.44(3)-0.53(1) mm/s, and the respective quadrupole splitting values were in the range of 0.62(6)-1.06(2) mm/s and 0.84(5)-1.07(1) mm/s. Although the resulting Mössbauer parameters confirmed that Fe in the *umoregi* wood was trivalent and its spin momentum number was 5/2 (i.e. high-spin state), no changes in spectral shape due to paramagnetic relaxation were observed even at 78 K. From this comprehensive investigation, it was determined that Fe^{3+} in Japanese oak and Japanese chestnut *umoregi* wood forms multinuclear complexes and has some differences in its first coordination sphere from Fe^{3+} in Japanese cedar and Japanese zelkova *umoregi* wood. Furthermore, it was suggested that the molecular structure of the Fe^{3+} complexes significantly affects the *umoregi* wood color tone.

1. Introduction

The Japanese term *umoregi* refers to ancient trees buried or submerged for a long period of time. In particular, this term implies that the trees, which have not been entirely denatured due to their isolation from sunlight and oxygen, were buried or submerged by natural phenomena (e.g., landslide, debris avalanche, ground subsidences) more than several hundred years ago. *Umoregi* generally refers to the trunk of the ancient trees. In English, bog wood, fossil wood (sub-fossil wood), and lignite have been used as translations for *umoregi*, however, they are not fully equivalent. This Japanese term does not belong to any scientific vocabulary and includes some ambiguity. In this study, we define *umoregi* wood as the trunk of an ancient buried tree that contains neither carbonized nor petrified components, although ancient trees are usually called *umoregi* even if they have undergone partial carbonization.

Most *umoregi* wood is brown or black in color, and sometimes deep green. Sufficiently sturdy *umoregi* wood can be used for construction and furniture, and they are traded as premium woody materials, because their characteristic colors or hues enhance their commercial value. The colors are due to chemical changes in the wood components that proceed slowly over a long period of time.

Umoregi trees have been found throughout Japan, and the degree of denaturation in them appears to be dependent on the tree species and the burial conditions, including the burial time and the soil type. In the last decade, Narita and co-workers have used chemical approaches to examine the essential oils contained in *umoregi* wood excavated in Japan.[1-5] However, these studies did not discuss the wood coloring mechanisms.

From studies of iron-gall ink[6-10] and dark spots on timber due to Fe contamination,[11-13] it has been recognized that the characteristic color of *umoregi* wood arises from reactions between Fe and polyphenols such as tannin. Only two studies[14, 15] on Fe in *umoregi* wood have been reported so far, and they made no mention of the coloring mechanism, although they investigated the chemical states of Fe in the wood using Mössbauer spectroscopy.

Our aim in this study is to determine the oxidation and spin state of Fe in *umoregi* wood and to obtain fundamental information about the molecular structure of Fe-containing chemical species. Here, we use ^{57}Fe Mössbauer spectroscopy and complementary analytical techniques to examine samples of *umoregi* wood obtained from trees excavated from the foothills of Mt. Chokai.

2. Experimental

2.1. *Umoregi* and raw wood samples. The *umoregi* trees used in this study were excavated in 2015 from Nikaho City in Akita Prefecture, Japan, located to the north-west of Mt. Chokai. The excavation site was within a construction area of the Nihonkai-Tohoku Expressway Nikaho interchange. It is conceivable that large-scale landslides occurred there and natural forests on the north-west side of Mt. Chokai to the present coast of Nikaho city were covered with soil and stone *ca.* 2500 years ago.[16, 17]

The *umoregi* trees were Japanese oak (OA; *Quercus* section *Prinus*, e.g. *Quercus serrata* or *Quercus crispula*), Japanese chestnut (CH; *Castanea crenata*), Japanese cedar (CE; *Cryptomeria japonica*), and Japanese zelkova (ZE; *Zelkova serrata*).

Hereafter, we refer to the tree trunks obtained by removing

*Corresponding author. E-mail: sigeru@iwt.akita-pu.ac.jp, Fax: +81-185-52-6924

Published on Web 01/25/2018

soil and bark from the excavated *umoregi* trees as "*umoregi* wood". After drying at ambient temperature for several months, *umoregi* wood was cut into *ca.* 9 × 9 × 1 cm^3 blocks. The trunk samples of OA (*Quercus serrata*), CH, CE, and ZE, which are modern species, were prepared to compare with *umoregi* wood samples. We refer to the trunks of the modern trees as "raw wood".

2.2. Treatment with oxalic acid. Oxalic acid is widely used as a timber bleaching agent for Fe contamination. It is generally accepted that the bleaching is due to formation of Fe oxalates instead of Fe tannates, because Fe oxalates exhibit a yellow or pale-yellow hue, and hence we treated the *umoregi* wood with oxalic acid solution. The *umoregi* wood blocks were cut into smaller blocks and dried in air at 105 °C for 24 hours in an electric oven. The small blocks were immersed in aqueous oxalic acid solution (3 w/w%), and the glass beaker holding the solution and blocks was subsequently placed in a vacuum desiccator. The internal pressure was sufficiently reduced using a water-jet pump, and the desiccator was sealed for 3 hours. The blocks were taken out from the solution and dried in air for more than 3 days. Special-grade oxalic acid was obtained from Wako Pure Chemical Industries, Ltd.

2.3. Preparation of sample powders for spectroscopic analyses. The small blocks of *umoregi* wood and raw wood were crushed to powder using a ceramic ball mill. Wood powder that could be passed through an 18.5-mesh-sieve was used as a sample for the spectroscopic measurements. Soil was collected at the excavation site of a ZE *umoregi* tree. The soil was ground in a ceramic mortar after air-drying, and the soil powder was analyzed by X-ray fluorescence spectrometry.

2.4. X-ray fluorescence spectrometry. Elements with atomic numbers greater than 11 in *umoregi* wood and soil samples were determined by X-ray fluorescence spectrometry using a compact spectrometer (MESA-500, Horiba, Ltd.). *Umoregi* wood (0.36 - 0.79 g) or soil (2.3 g) powder was placed in a cylindrical polytetrafluoroethylene cell with a diameter of 20 mm. The sample chamber was evacuated using an oil-sealed rotary vacuum pump during measurements. X-ray irradiation was done at room temperature and the total measurement time was 2000 s. The X-ray tube voltages were 15 kV (1000 s) and 50 kV (1000 s). Relative mass percentages of elements to total elements detected were estimated using a standardless fundamental parameter method[18, 19] from characteristic X-ray intensities.

2.5. Infrared photoacoustic (IR-PA) spectroscopy. The IR-PA spectra were obtained at 22±1 °C using a spectrometer (JIR7000W, JEOL, Ltd.) equipped with an IR-PA spectroscopy module (IR-PAS 1000, JEOL, Ltd.). The spectra were obtained from 300 accumulations with a spectral resolution of *ca.* 4 cm^{-1}. A thin cell (diameter, 5 mm) was filled with the wood powder, and photoacoustic signals were collected upon purging a cell bench with He gas. The moving-mirror velocity was fixed at 0.16 cm/s. Carbon black was used as a reference.

2.6. Mössbauer spectroscopy. ^{57}Fe Mössbauer measurements were carried out in a conventional transmission mode on a Mössbauer spectrometer (Model-222, Topologic System Co.) with a ^{57}Co(Rh) source (925 MBq). Measurement temperatures were 293 K and 78 K and they were regulated using an Oxford cryostat DN-1726 with an ITC-601 temperature controller. Curve fitting of the Mössbauer spectra was performed by a nonlinear least-squares method using the MossWinn 4.0Pre. program, assuming that all spectra were composed of a doublet of Lorentzian-shaped peaks. The isomer shift (IS) and Doppler velocity scale were calibrated with respect to the sextet of α-Fe at room temperature.

The *umoregi* wood sample thicknesses of CE and the other three were *ca.* 43 mg/cm^2 and *ca.* 30 mg/cm^2, respectively, and these allowed us to discuss Mössbauer absorption intensities semi-quantitatively.

3. Results and Discussion

3.1. *Umoregi* wood colors and bleaching with oxalic acid treatment. Figure 1 shows photos of the *umoregi* and raw wood samples, and the *umoregi* wood samples treated with

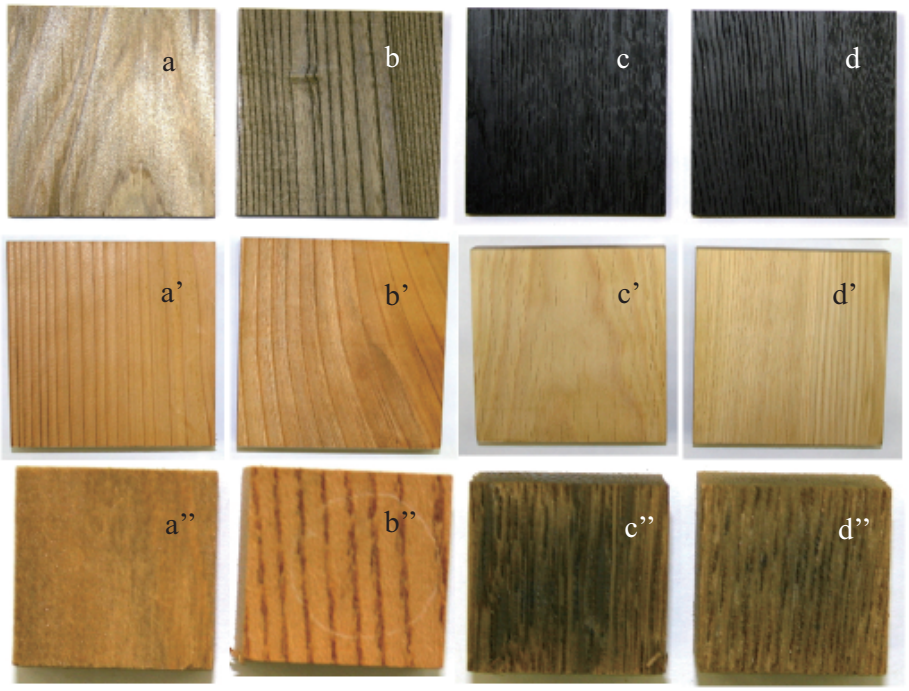

Figure 1. *Umoregi* and raw wood samples, and *umoregi* wood samples treated with oxalic acid. The top row is *umoregi* wood (a, CE; b, ZE; c, OA; d, CH), the middle row is raw wood (a', CE; b', ZE; c', OA; d', CH), and the bottom row is *umoregi* wood treated with oxalic acid (a'', CE; b'', ZE; c'', OA; d'', CH).

TABLE 1: Relative mass percentage of elements in *umoregi* wood and soil samples

Sample	Element wt%										Ash content %
	Mg	Al	Si	P	S	Cl	K	Ca	Mn	Fe	
CE* *umoregi*	-	2.0(1)	12.8(1)	0.2(1)	-	0.3(2)	1.1(1)	39.9(2)	1.9(1)	41.2(2)	0.62
ZE* *umoregi*	-	1.4(2)	22.4(2)	0.5(1)	-	1.4(2)	1.0(1)	34.0(2)	0.1**	38.6(2)	1.38
OA* *umoregi*	-	4.8(1)	11.7(1)	-	13.5(1)	-	0.8**	14.4(1)	1.0**	53.7(1)	1.31
CH* *umoregi*	-	0.7**	4.4**	-	-	-	1.1**	21.5(1)	0.3**	72.1(1)	2.73
Soil***	2.2**	11.6(1)	61.5(1)	-	1.2**	-	4.5**	4.2**	0.2**	13.3**	-

*CE, Japanese cedar; ZE, Japanese zelkova; OA, Japanese oak; CH, Japanese chestnut.
**Standard deviation is less than 0.1.
***Gray soil was present at the excavation site of the ZE *umoregi* tree.

oxalic acid. In the top row, CE and ZE *umoregi* wood appeared as brown (khaki) and dark green (olive green), respectively. *Umoregi* wood of OA and CH, which belong to the family of *Fagaceae*, exhibited a pure black tone. Therefore, the colors of *umoregi* wood may vary with wood species. By comparing with the raw wood shown in the middle row, we saw that the wood color changed drastically with the burial time, and the color of *umoregi* wood was unrelated to that of the raw wood.

The *umoregi* wood samples shown in Figure 1 were prepared about 15 months after tree excavation, and their Mössbauer and IR-PA spectra were recorded at roughly the same time. The color tones of CE and ZE *umoregi* wood had changed to brown and dark green, respectively, immediately after the excavation. However, we judged that their color tones slightly and gradually became deeper with time. As for OA and CH *umoregi* wood, no color tone changes with time could be observed by the naked eye.

As mentioned above, although no studies are available on the coloring mechanism of *umoregi* wood based on immediate evidence, it is commonly recognized that the color features of *umoregi* wood are due mainly to Fe compounds interacting with polyphenols such as tannin. This has been deduced from studies of the historical ink (iron-gall ink)[6-10] or stains on timber caused by Fe contamination.[11-13] The stains showed dark colors similar to those of *umoregi* wood. Moreover, it has been reported that the dark stains occur on timber owing to Cu, Cr, and Mn as well as Fe.[20-22]

The bottom row shown in Figure 1 presents *umoregi* wood pieces treated with oxalic acid which were cut from the *umoregi* wood blocks shown in the top row. In all the *umoregi* wood pieces, their characteristic colors vanished dramatically through this treatment. The CE and ZE *umoregi* wood turned colors close to those of their raw wood, and the pure black tone faded away from the OA and CH *umoregi* wood. From the disappearance of dark color, we anticipated that the coloring mechanisms in *umoregi* wood were similar to those in timber caused by Fe contamination.

3.2. Elements analysis of *umoregi* wood and soil samples. Table 1 summarizes the relative mass percentage of elements from Mg to Pb in *umoregi* wood and soil samples collected from the excavation site.

Tsuchiya et al.[23] reported the content of minor elements in the wood and bark of various raw tree species including CE, ZE, and OA using inductively coupled plasma emission spectrometry. Wood and bark are organic matter, and the major elements constituting them are C, O, and H. According to their study, K and Ca were major elements among metals, exceeding 1000 mg/kg in more than half of the wood samples. Mg, Si, and P were classified into a secondary group among the minor elements and their contents ranged from dozens to several hundred mg/kg. The Fe content in the wood samples was under 10 mg/kg and less than Al and Sr.

The *umoregi* wood had not been degraded markedly as mentioned later, and hence C, O, and H should also be major elements. In contrast, Fe was a major element in all the *umoregi* wood samples among the elements detected using X-ray fluorescence spectrometry, and, in particular, the relative mass percentage of Fe in CH *umoregi* wood was more than 70%. The elemental analysis indicated that Fe content in the soil was much higher than that in the raw wood samples. Thus, it can be assumed that Fe was transferred from the soil to the *umoregi* wood during the long burial period. Other transition metals, which are capable of causing color changes in *umoregi* wood, were negligible except for Mn. Although the contents of Mn were larger than those of Cu, Ni, or Pb, particularly in CE and OA *umoregi* wood, the relative mass percentages of Mn were an order of magnitude lower than those of Fe. Most Ca contained in the *umoregi* wood was expected to have been already present in the trees when they were buried.

We noted that the relative mass percentages of Al in the *umoregi* wood were much less than those of Fe despite the value of Al being close to that of Fe in the soil sample. This might be explained as follows. In general, Al^{3+} shows many similarities in chemical behavior to Fe^{3+} and all of the Al contained in the soil must be trivalent (Al^{3+}). However, our previous Mössbauer measurement revealed that the Fe^{2+}/Fe^{3+} ratio in the soil was *ca*. 3/7,[24] and therefore Fe^{2+} might transfer to *umoregi* wood more easily than Fe^{3+}.

Major elements of raw wood are C, O, and H, as mentioned above, and the sum of their contents is about 99 %. These elements cannot be detected by X-ray fluorescence spectrometry. Thus, the relative mass percentages shown in Table 1 should be much larger than the absolute mass percentages. We adopted a simple calculation method to estimate roughly the absolute mass percentage of Fe in the *umoregi* wood samples. In particular, assuming that only elements with atomic numbers smaller than 11 were completely removed from ash by burning, we calculated the tentative absolute mass percentages of Fe based on Eq. (1):

$$TP_{Fe} = RP_{Fe} \times A \times 1/100 \quad (1)$$

where TP_{Fe}, RP_{Fe}, and A are the tentative absolute mass percentage, relative mass percentage, and ash content in a percent unit, respectively. The ash contents of CE, ZE, OA, and CH *umoregi* wood samples were 0.62, 1.38, 1.31, and 2.73%, respectively, as reported in our previous work.[24] The TP_{Fe} values obtained from Eq. (1) of CE, ZE, OA, and CH *umoregi* wood samples were approximately 0.3, 0.5, 0.7, and 2%, respectively.

Eq. (1) is an approximate calculation because metal elements should be contained as oxides in ash. We expect, however, that TP_{Fe} obtained from Eq. (1) is a useful tool to estimate the chemical states of Fe in the *umoregi* wood.

3.3. Infrared photoacoustic (IR-PA) spectroscopy. Figure 2 depicts the IR-PA spectra over the 2000 - 750 cm^{-1} range of the *umoregi* and raw wood samples. It is difficult to obtain a fine IR spectrum from black or dark-colored samples such as degraded wood and charcoal using ordinary techniques because of non-resonant absorption. Photoacoustic spectroscopy is a suitable technique to measure the IR spectra of such samples. For example, by means of the IR-PA spectroscopic technique, we have studied the weathering of tropical woods, revealing that this method is a useful tool to follow chemical changes in functional groups, especially carbonyl, carboxyl, and phenyl groups.[25]

As seen in Figure 2, the IR-PA spectrum of the *umoregi* wood samples was analogous to that of the same species of raw wood except for the regions of 1800 - 1620 cm^{-1} and 1300 - 1200 cm^{-1}. We noted that there were no significant spectral differences between raw and *umoregi* wood samples in the vibrational bands due to phenyl groups of lignin (1592 cm^{-1} and 1503 cm^{-1}) [26, 27] and saturated cyclic groups of cellulose or hemicellulose (1450 - 1320 cm^{-1} and 1180 - 1000 cm^{-1}, respectively).[26] Therefore, we could assume that the degradation of *umoregi* wood had not proceeded drastically during the 2500-year-burial of these trees.

Remarkable spectral differences, however, appeared in two regions. A broad band around 1740 cm^{-1} was assigned mainly to C=O stretching vibrations in carboxyl[26] and unconjugated carbonyl[28] groups, and the band intensity of *umoregi* wood was much less than that of raw wood. The band of stretching vibrations attributed to conjugated C=O groups[28] was detected at *ca.* 1650 cm^{-1}, and its intensity in *umoregi* wood seemed to be slightly less than in raw wood. Furthermore, it seemed that the band intensities in the region of 1300 - 1200 cm^{-1} for the *umoregi* wood samples except for CE were smaller than those of the raw wood samples. Several vibrational modes have bands in this region and one of them will be a stretching vibration of C-O in carboxyl groups.[26] Thus, the IR-PA spectra of the *umoregi* wood samples reinforced the suggestion that some chemical changes occurred in carboxyl and/or carbonyl groups during the long burial period.

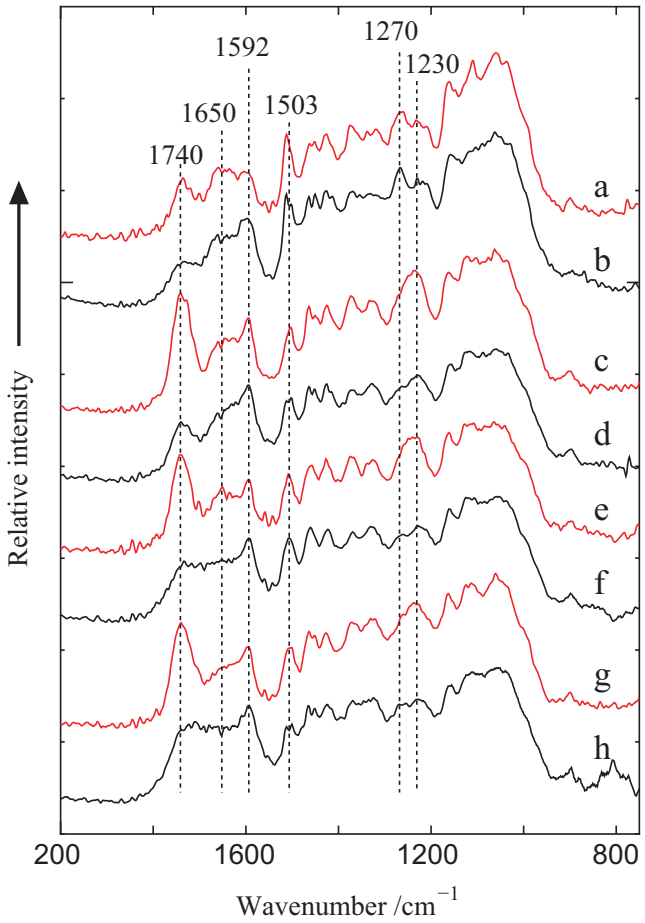

Figure 2. IR- PA spectra of raw and *umoregi* wood samples: a, CE (raw wood); b, CE (*umoregi* wood); c, ZE (raw wood); d, ZE (*umoregi* wood); e, OA (raw wood); f, OA (*umoregi* wood); g, CH (raw wood); h, CH (*umoregi* wood).

There are two possible chemical changes. One is decomposition of the functional groups, and the other is the occurrence of chemical interactions between the functional groups and their neighboring species. If O atoms included in the functional groups form hydrogen, ionic or coordinate bonds, the bands at 1740 and 1650 cm^{-1} would be shifted to considerably lower wavenumbers.[29] It was, however, difficult to determine from the IR-PA spectra whether such shifts occurred.

3.4. Mössbauer spectroscopy. Figures 3 and 4 show the Mössbauer spectra of *umoregi* wood samples recorded at 293 K and 78 K, respectively. The absorption intensities are substantially weak for almost all *umoregi* wood samples because of the low Fe contents (0.3 to 2 %) as described in Section 3.2. Absorption lines in all the Mössbauer spectra consisted of a set of doublet lines, and no magnetic hyperfine splitting was observed even at 78 K. Table 2 summarizes the Mössbauer parameters (IS; quadrupole splitting, QS; and line width, LW) calculated by curve fitting. The LW values were slightly but clearly larger (~0.26 mm/s in the present work) compared with ordinary Fe compounds. This enhancement of LW is explained later. In addition, from Figures 3 and 4, the Mössbauer absorption intensity was considered to be in the following order: CE < ZE < OA < CH, and this was in agreement with the order of TP_{Fe} (see Section 3.2).

The IS values of 0.21 to 0.43 mm/s at 293 K indicated that Fe in all of the *umoregi* wood samples was high-spin Fe^{3+} or low-spin Fe^{2+}.[30-32] The assignment to high-spin Fe^{2+} should be excluded, since the IS and QS values at 293 K (Table 2) ranged from 0.2 mm/s to 0.5 mm/s and from 0.6 mm/s to 1.1 mm/s, respectively, and they were much smaller than those of most high-spin Fe^{2+} compounds.[33, 34] It seemed that all the IS and QS values at 293 K of Fe in the *umoregi* wood samples were within the shared ranges between high-spin Fe^{3+} and low-spin Fe^{2+}.[33, 34] However, the assignment to low-spin Fe^{2+} should also be excluded, because the *umoregi* wood and soil samples would contain little or no amounts of ligands inducing a large ligand field splitting such as CN^-, NO_2^-, or NH_3. Therefore, the Fe in the *umoregi* wood samples was most likely to be high-spin Fe^{3+}. However, the QS values were somewhat larger than values typically seen for high-spin Fe^{3+} compounds.

The four types of *umoregi* wood were classified into two groups based on their IS and QS, as shown in Figure 5. Group 1 consisted of CE and ZE, and Group 2 consisted of OA and CH. IS and QS of Group 1 were significantly smaller than those of Group 2. Moreover, the two groups differed from each other in color; Group 1 samples were brown or dark green, while Group 2 samples were pure black as seen in Figure 1. Hence, the first coordination sphere of Fe in Group 1 would be expected to be somewhat different from that in Group 2, even though Fe in both groups exists as high-spin Fe^{3+} species.

Group 1 showed a small but clear temperature-dependence for QS, although the QS values of Group 2 were independent of temperature. This suggested that Fe^{3+} species in Group 1 may undergo some structural change from 293 K to 78 K, because QS of high-spin Fe^{3+} shows little or no temperature-depndence.[31] Moreover, the differences in IS of Group 2 between 293 K and 78 K were *ca.* 0.1 mm/s as shown in Table 2, which was consistent with the second-order Doppler shift.[30] However, the increases in IS of Group 1 at 78 K were too large to be accounted for as the second-order Doppler shift alone,

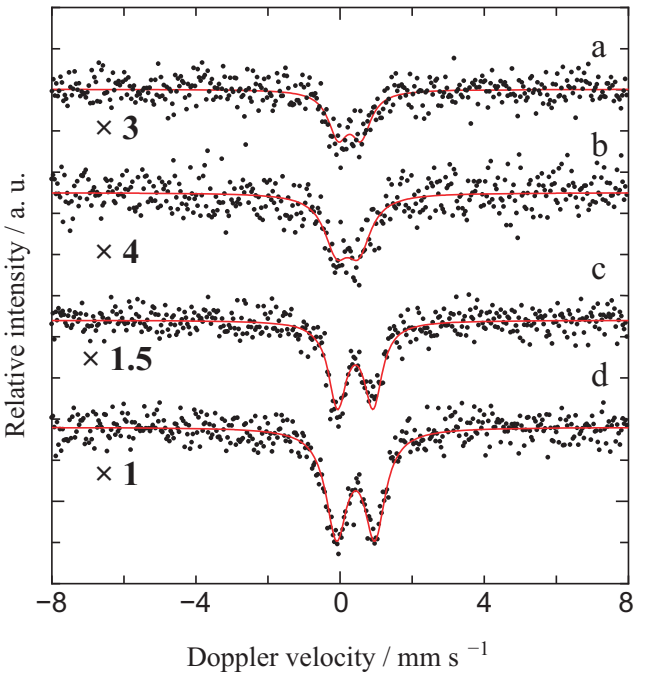

Figure 3. Mössbauer spectra at 293 K of *umoregi* wood samples: a, CE; b, ZE; c, OA; and d, CH. Numerals in the spectra represent a relative magnification of intensity when the spectrum of CH is used as a reference. The percent absorption intensity is about 0.8 % at the maximum for CH.

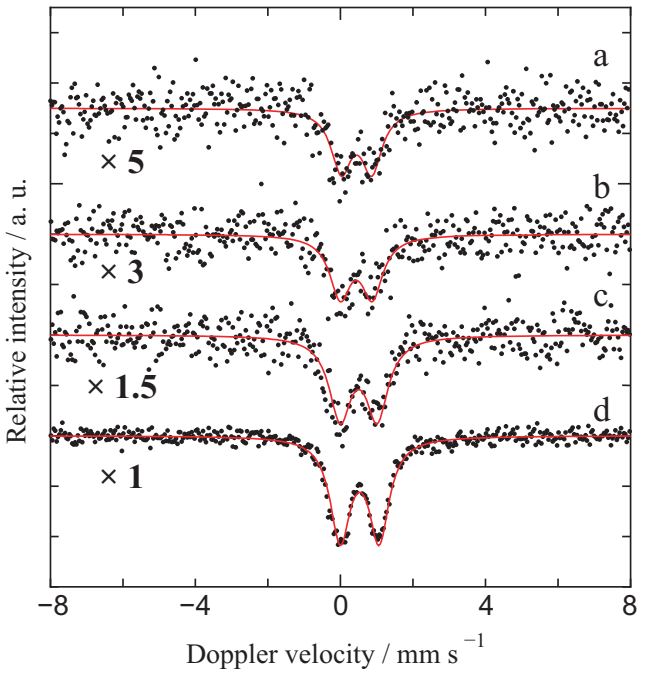

Figure 4. Mössbauer spectra at 78 K of *umoregi* wood samples: a, CE; b, ZE; c, OA; and d, CH. Numerals in the spectra represent a relative magnification of intensity when the spectrum of CH is used as a reference. The percent absorption intensity is about 1.6 % at the maximum for CH.

TABLE 2: Mössbauer parameters of *umoregi* wood samples

Umoregi wood sample	Temp. K	IS** mm s^{-1}	QS*** mm s^{-1}	LW**** mm s^{-1}
CE*	293	0.26(3)	0.64(5)	0.66(8)
	78	0.44(3)	0.84(5)	0.68(7)
ZE*	293	0.21(3)	0.62(6)	0.82(15)
	78	0.44(3)	0.88(4)	0.70(7)
OA*	293	0.42(1)	0.99(2)	0.60(3)
	78	0.51(1)	0.98(1)	0.70(2)
CH*	293	0.43(1)	1.06(2)	0.70(3)
	78	0.53(1)	1.07(1)	0.67(1)

*CE, Japanese cedar; ZE, Japanese zelkova; OA, Japanese oak; CH, Japanese Chestnut.
**Isomer shift, ***quadrupole splitting, ****line width.

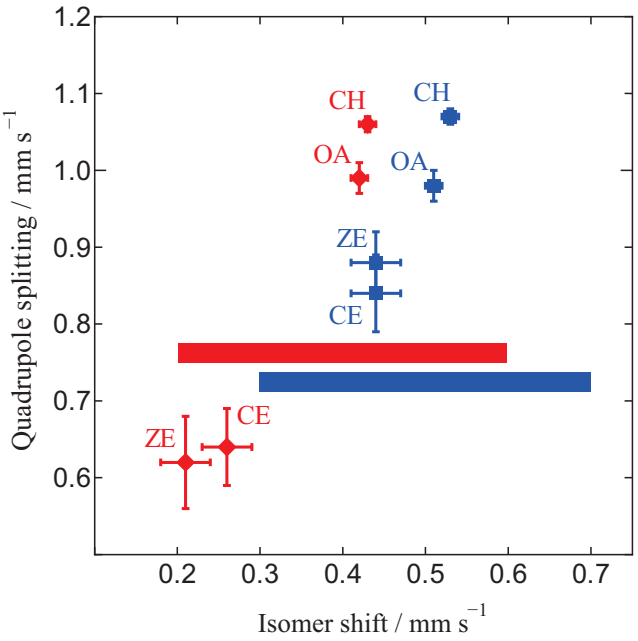

Figure 5. Isomer shift and quadrupole splitting at 293 K (♦) and 78 K (■) of Fe in *umoregi* wood samples. The red band shows the IS range for high-spin Fe^{3+} at room temperature[32, 34], and the blue band shows that at liquid nitrogen temperature estimated from the second-order Doppler shift[30] on the basis of the former range.

and it appeared that there was some structural change taking place between 293 K and 78 K.

It is well recognized, at room temperature, that IS is in the range of 0.3 – 0.6 mm/s if coordinating atoms to Fe^{3+} form an octahedron (six-coordinated structure), and in the range of 0.2 – 0.4 mm/s if a tetrahedron (four-coordinated structure) is formed.[32] The IS of Fe^{3+} in Group 2 *umoregi* wood samples was in the former range, whereas the IS of Fe^{3+} in Group 1 *umoregi* wood samples was slightly less than 0.3 mm/s. It is, however, known that most Werner type Fe^{3+} complexes have an octahedral coordination geometry, except for halogeno-complexes.

On the other hand, for high-spin Fe^{3+} species, it has been reported that QS ranges at room temperature corresponding to the six-coordinated and four-coordinated structure ranges are approximately 0 – 1.1 mm/s and 0 – 0.75 mm/s, respectively.[34] As listed in Table 2, our QS values supported the finding that the coordination number of Fe^{3+} in Group 2 *umoregi* wood samples was six; however, they did not suggest a coordination number of Fe^{3+} in Group 1 *umoregi* wood samples.

Accordingly, the Fe^{3+} in Group 2 *umoregi* wood is certainly located at the center of an octahedron structure. In contrast, it is difficult to determine from Mössbauer parameters whether the first coordination sphere of Fe^{3+} in Group 1 *umoregi* wood is a tetrahedral or octahedral structure.

Several studies have addressed the reaction between Fe and polyphenols, and discussed the structure of polyphenol-Fe complexes. These studies are divided into two categories. The first is research into the effects of polyphenols in wood on

Fe corrosion.[6-10] Researchers have supposed that two kinds of mononuclear Fe(III) complexes bonded to tannins as a bidentate ligand are formed by the reaction with tannins extracted from wood, on the basis of Mössbauer spectroscopic analysis. The second category is a series of studies of historical ink (iron-gall ink).[35-37] From both categories, it should be noted that a basic structure for a model compound for gallic acid-Fe(III) complex was determined using an X-ray diffraction method.[6, 37] The gallic acid-Fe(III) complex has polynuclear structures, and a molecule of gallic acid forms three bonds between its three hydroxyl groups and two Fe atoms, and a chelate bond between its carboxyl group and another Fe atom. Fe atoms are located at the center of the octahedral structures. However, it will be very difficult to determine the structure of Fe compounds contained in the *umoregi* wood samples by X-ray diffraction methods, because Fe concentrations are low and the crystals are microscopical if Fe compounds are crystallized.

Our Mössbauer data suggested that Fe species in Group 2 *umoregi* wood had multinuclear structures for which a unit contained two or more Fe atoms, because no changes in spectral shape due to paramagnetic relaxation were observed even at 78 K despite the presence of high-spin Fe^{3+}. However, it was difficult from our Mössbauer spectral data to determine whether or not their molecular structures were analogous to that of the gallic acid-Fe(III) complex.

Paramagnetic relaxation phenomena in Mössbauer spectroscopy have been interpreted as the fluctuation of magnetic fields produced by electronic spins in paramagnetic compounds, and the fluctuation rate decreases as temperature decreases. This phenomenon is observable in high-spin Fe^{3+} and Eu^{2+} whose orbital momentum vanishes ($L \approx 0$) as changes in Mössbauer spectra. Well-resolved magnetic hyperfine splitting clearly appears in Mössbauer spectra when a fully fixed magnetic field exists at a Mössbauer nuclide. Meanwhile, a magnetic field has no influence on Mössbauer absorption line-shape if its fluctuations are sufficiently fast. In both cases, Mössbauer spectra can be expressed as a combination of Lorentzian curves. However, at intermediate spin fluctuation rates comparable to the Larmor precession rate of the Mössbauer nucleus, it is known that the Mössbauer absorption line-shape becomes complicated through the relaxation effect and cannot be precisely approximated with Lorentzian or Gaussian curves.[30]

We previously reported the Mössbauer spectra of high-spin Fe^{3+} [38-43] and Eu^{2+} [44, 45] compounds and their frozen solutions, and indicated that the electron-spin fluctuation rate decreases as the Fe-Fe or Eu-Eu distance increases due to less spin-spin dipole interaction. Specifically, we experimentally examined the Mössbauer line-shapes of tris(β-diketonato)Fe(III)[38, 39] and hexakis(alkylurea)Fe(III)[42] complexes, which have a six-coordinate octahedral structure in terms of the paramagnetic relaxation effect. The Mössbauer spectra of all these complexes showed an apparent single absorption line, but the line had wings on both sides and its line-shape was distinctly non-Lorentzian. The bulkier the ligand of the Fe complex, the larger the wings were. In other words, the absorption line-shape broadened with increasing average Fe-Fe distance in the complexes. The absorption line at liquid nitrogen temperature (78K) exhibited more obvious broadening compared with that at room temperature in each complex. Moreover, splittings due to magnetic hyperfine structures were observed in the Mössbauer spectra when $Fe(III)(acac)_3$ (acac, $CH_3COCHCOCH_3^-$) complexes were homogeneously dispersed in frozen solutions.[38, 40]

In contrast, it was confirmed that the Mössbauer absorption line-shape of $[(\mu\text{-}CH_3O)Fe(III)(dpm)_2]_2$ (dpm, $(CH_3)_3COCHCOCH(CH_3)_3^-$), which is a dinuclear Fe complex, shows no significant changes when dispersed in a frozen solution despite the fact that the Fe^{3+} in the complex is in the high-spin state and located at the center of an octahedral structure.[46] This was interpreted as an indication that the spin-spin dipole interaction was hardly weakened by dispersion in frozen solution, because the Fe-Fe distance in the dinuclear Fe complex unit was constant.

Accordingly, the Mössbauer absorption line of Fe in Group 2 *umoregi* wood samples should exhibit broad wings or some differences from Lorentzian curves if the Fe^{3+} species were mononuclear complexes. The reasons are as follows.

(1) Fe^{3+} species in Group 2 *umoregi* wood certainly have six-coordinate octahedral structures.

(2) Polyphenols, which will be bulkier than β-diketone and alkylurea molecules, likely form chemical bonds with Fe^{3+} as ligands.

In addition, the wings at 78 K should be broader and larger than those at 293 K. Nevertheless, neither wings nor differences from Lorentzian curves were observed in the Mössbauer absorption of Fe in the *umoregi* wood samples and the absorption lines shown in Figures 3 and 4 were well explained by a superposition of two identical Lorentzian curves.

The wood components with pyrogallol groups that can form cross-linked structures by an O-Fe-O-Fe-O bond include several polyphenols containing tannins. As a result of the Mössbauer spectroscopic measurements, we concluded that Fe^{3+} formed multinuclear complexes with polyphenols in Group 2 *umoregi* wood. Furthermore, the large LW values allowed us to predict co-existence of two or more kinds of Fe complexes with similar structures, and this prediction was applicable to Group 1 *umoregi* wood.

On the other hand, the absence of a paramagnetic relaxation effect on the Mössbauer absorption line-shape could not be easily accepted as evidence that Fe^{3+} species in Group 1 *umoregi* wood were multinuclear complexes, because the coordination atoms to Fe^{3+} may form tetrahedral structures.

Our Mössbauer spectroscopic data indicated that Fe^{3+} species in Group 1 *umoregi* wood differ significantly from those in Group 2 *umoregi* wood in terms of their molecular structure, thereby reinforcing the suggestion that the molecular structure of Fe^{3+} species is an important factor determining the color tone of the *umoregi* wood. Further study is necessary to understand completely the molecular structures of Fe^{3+} species in different types of *umoregi* wood.

4. Conclusion

The results of the Mössbauer spectroscopic analysis described here confirmed that Fe in the *umoregi* wood samples had a $3d^5$ electron configuration and its spin quantum number (S) was 5/2 (high-spin state), and they indicated that the high-spin Fe^{3+} species in OA and CH *umoregi* wood samples exhibited octahedral symmetry and could be attributed to multinuclear compounds. Moreover, the temperature-dependence of IS and QS suggested that some structural changes might occur in Fe^{3+} species in CE and ZE *umoregi* wood samples between 293 K and 78 K.

Comprehensive investigation of all the experimental results indicated that the Fe^{3+} complexes included polyphenols with pyrogallol groups as ligands, and suggested that their molecular structure was a governing factor for the *umoregi* wood color tone.

Acknowledgement

We are grateful to the Nikaho City Board of Education for the donation of the *umoregi* wood samples.

References

(1) H. Narita, M. Yatagai, and T. Ohira, J. Essent. Oil Res. **18**, 68(2006).
(2) H. Narita, and M. Yatagai, Org. Geochem. **37**, 818 (2006).
(3) H. Narita, K. Huruhata, S. Kuga and M. Yatagai, Phytochem. **68**, 587(2007).
(4) H. Narita, Mokuzai Kogyo **68**, 330(2013).
(5) H. Narita, Wood Protection **42**, 62(2016).
(6) C. H. Wunderlich, R. Weber, and G. Bergerhoff, Z. anorg. allg. Chem. **598/599**, 371(1991).
(7) C. Krekel, Int. J. For. Doc. Exam. **5**, 54(1999).
(8) B. Wagner, E. Bulska, B. Stahl, M. Heck, and H. M. Ortner, Anal. Chim. Acta **527**, 195(2004).
(9) C. Burgaud, V. Rouchon, P. Refait, and A. Wattiaux, Appl. Phys. **A92**, 257(2008).
(10) C. Canevari, M. Delorenzi, C. Invernizzi, M. Licchelli, M. Malagodi, T. Rovetta, and M. Weththimuni, Wood Sci. Technol. **50**, 1057(2016).
(11) W. Sandermann, and M. Lüthgens, Holz als Roh-u. Wérkst. **11**, 435(1953).
(12) T. Kondo, H. Uto, and M. Suda, Mokuzai Gakkaishi **2**, 221(1956).
(13) K. Takenami, Mokuzai Gakkaishi **10**, 22(1964).
(14) S. Yamauchi, Y. Sakai, and H. Aimi, J. Wood Sci. **57**, 549(2011).
(15) U. Bürck, F. E. Wagner, and A. Lerf, Hyperfine Interact. **208**, 105(2012).
(16) H. Sakurai, W. Kato, Y. Takahashi, K. Suzuki, Y. Takahashi, S. Gunji, and F. Tokanai, Radiocarbon **48**, 401(2006).
(17) S. Hayashi, Sabo & Chisui **45**, 80(2012).
(18) A. Kira, and N. Robson, Readout No. 22, 19(2001).
(19) W. T. Elam, R. B. Shen, B. Scruggs, and J. Nicolosi, Adv. X-ray Anal. **47**, 104(2004).
(20) J. Wehrmann, Holz als Roh-u. Wérkst. **15**, 325(1957).
(21) L. Plath, Holz als Roh-u. Wérkst. **16**, 357(1958).
(22) K. Takenami, Mokuzai Gakkaishi, **10**, 30(1964).
(23) Y. Tsuchiya, H. Shimogaki, H. Abe, and A. Kagawa, J. Wood Sci. **56**, 53(2010).
(24) S. Yamauchi, Y. Kurimoto, and Y. Sakai, J. Nucl. Radiochem. Sci. **17**, 1(2017).
(25) S. Yamauchi, Y. Sudiyani, Y. Imamura, and S. Doi, J. Wood Sci. **50**, 433(2004).
(26) A. J. Michell, A. J. Watson, and H. G. Higgins, Tappi **48**, 520(1965).
(27) U. M. Agarwal, J. D. McSweeny, and S. A. Ralph, J. Wood Chem. Tech. **31**, 324(2011).
(28) I. R. Lewis, N. W. Daniel, N. C. Chaffin, Jr., and P. R. Griffiths, Spectrochim. Acta **50A**, 1943(1994).
(29) K. Nakamoto, *Infrared and Raman spectra of inorganic and coordination compounds Part B: Applications in coordination, organometallic, and bioinorganic chemistry*, A John Wiley & Sons, Inc., New Jersey, (2009).
(30) P. Gütlich, E. Bill, and A. X. Trautwein, *Mössbauer spectroscopy and transition metal chemistry -Fundamentals and applications*-, Springer-Verlag, Berlin, (2011).
(31) J. C. Travis, *The electric field gradient tensor*, in: *An introduction to Mössbauer spectroscopy* Ed. L. May, Plenum Press, New York, (1971).
(32) F. Menil, J. Phys. Chem. Solids, **46**, 763(1985).
(33) N. N. Greenwood, and T. C. Gibb, *Mössbauer spectroscopy*, Chapman and Hall Ltd., London, (1971).
(34) R. E. Vandenberghe, and E. De Grave, *Mössbauer spectroscopy*, Eds. Y. Yoshida, and G. Langouche, Springer-Verlag, Berlin, (2013).
(35) J. Gust, and J. Suwalski, Corrosion **50**, 355(1994).
(36) J. A. Jaén, J. De Obaldía, and M. V. Rodríguez, Hyperfine Interact. **202**, 25(2011).
(37) R. K. Feller, and A. K. Cheetham, Solid State Sci. **8**, 1121(2006).
(38) Y. Sakai, H. Nishioji, S. Yamauchi, and T. Tominaga, Radiochem. Radioanal. Lett. **53**, 215(1982).
(39) S. Yamauchi, Y. Sakai, and T. Tominaga, Int. J. Appl. Radiat. Isot. **34**, 977(1983).
(40) Y. Sakai, H. Nishioji, and T. Tominaga, Radiochim. Acta **36**, 181(1984).
(41) S. Yamauchi, Y. Sakai, and T. Tominaga, Bull. Chem. Soc. Jpn. **58**, 442(1985).
(42) S. Yamauchi, Y. Sakai, and T. Tominaga, J. Radioanal. Nucl. Chem. Lett. **119**, 283(1987).
(43) S. Yamauchi, Y. Sakai, and T. Tominaga, J. Radioanal. Nucl. Chem. Lett. **146**, 185(1990).
(44) S. Yamauchi, Y. Minai, and T. Tominaga, J. Radioanal. Nucl. Chem. Lett. **93**, 238(1985).
(45) S. Yamauchi, T. Watanabe, and T. Tominaga, Radiochim. Acta **43**, 51(1988).
(46) S. Yamauchi, *Mössbauer spectroscopic study of magnetic relaxation in iron compounds*, The University of Tokyo, 1983, Master's thesis.